*Quaternary Research* (2017), **87**, 455–467.

doi:10.1017/qua.2017.9

# Holocene climatic and environmental change on the western Tibetan Plateau revealed by glycerol dialkyl glycerol tetraethers and leaf wax deuterium-to-hydrogen ratios at Aweng Co

Xiumei Li[a,b], Mingda Wang[a], Yuzhi Zhang[c], Li Lei[d], Juzhi Hou[a,d]*

[a]Key Laboratory of Tibetan Environment Changes and Land Surface Processes, Institute of Tibetan Plateau Research, Chinese Academy of Sciences, Beijing 100101, China
[b]University of Chinese Academy of Sciences, Beijing 100049, China
[c]Key Laboratory of West China's Environmental System (Ministry of Education), Lanzhou University, Lanzhou 730000, China
[d]School of Earth Sciences, China University of Geosciences, Wuhan 430074, China

(Received February 23, 2016; Accepted January 18, 2017)

**Abstract**

Mean annual air temperature (MAAT) and precipitation isotope records for the Holocene were obtained from the analysis of the relative distribution of branched glycerol dialkyl glycerol tetraethers and compound-specific hydrogen isotope ratios of leaf waxes from a sediment core from Aweng Co on the western Tibetan Plateau (WTP). Our results indicate that the Indian monsoon mainly influenced Aweng Co during the Holocene. During the early Holocene, when summer insolation was at a maximum, the monsoonal influence was strong and the climate was warm and wet. Both the summer and winter insolation were relatively weak, and Aweng Co was cool and dry during the middle Holocene (6–3 ka), indicating a weakening of the Indian monsoon. The southward displacement of the Intertropical Convergence Zone and relatively low atmospheric methane content may have contributed to the middle Holocene cooling on the WTP. During the late Holocene, with a further increase in winter insolation and decrease in summer insolation, the summer monsoon weakened and the MAAT on the WTP gradually increased. Depleted leaf wax hydrogen isotope ratios during the late Holocene can be attributed to accelerated glacier melting because of the elevated MAAT.

**Keywords:** Tibetan Plateau; Aweng Co; Holocene; Indian summer monsoon; GDGTs; Sedimentary leaf waxes

## INTRODUCTION

The Tibetan Plateau is often referred to "Asia's Water Tower" as it hosts continental glaciers of a size exceeded only by those of Antarctica and Greenland. Almost all of the major rivers in East and South Asia originate from the glaciers on the Tibetan Plateau, which provide freshwater resources to more than one-third of the world's population (Immerzeel, 2008; Immerzeel et al., 2010). Therefore, the future behavior of the glaciers on the Tibetan Plateau is of great importance given their potential effects on the region's hydrology and thus the human population. Over the past few decades, glacier accumulation on the Tibetan Plateau has been affected by changing precipitation patterns (Yao et al., 2012). In the southern and eastern Tibetan Plateau, the glaciers have retreated as a result of the decreased influence of monsoonal precipitation, whereas glacier accumulation in the western Tibetan Plateau (WTP) has increased because of the climatic influence of the midlatitude westerlies (Yao et al., 2012). In addition to precipitation, temperature also plays a critical role in the stability of these glaciers (Bradley et al., 2006). Meteorological observations on the Tibetan Plateau over the past few decades provide evidence of more pronounced regional warming compared with the global average (Liu et al., 2009), which is consistent with climate modeling results that indicate that temperature varies more significantly at higher elevations than at lower elevations (Bradley et al., 2004, 2006). Clearly, an increased number of long, continuous, and quantitative paleotemperature records are essential for understanding past changes in the glaciers on the Tibetan Plateau.

The climate of the Tibetan Plateau is influenced by the East Asian monsoon, the Indian monsoon, and the midlatitude westerlies. The extent of monsoonal influence on the Tibetan Plateau is modulated by the average position of the midlatitude westerly jet (Schiemann et al., 2009;

*Corresponding author at: Key Laboratory of Tibetan Environment Changes and Land Surface Processes, Institute of Tibetan Plateau Research, Chinese Academy of Sciences, Beijing 100101, China. E-mail address: houjz@itpcas.ac.cn (J. Hou).

Chiang et al., 2015). Combining precipitation isotope records and temperature records is likely to be important for understanding changes in the extent of monsoonal influence on the Tibetan Plateau. In addition, there is debate about Holocene temperature variations between proxy indicators and models. The former show temperature gradually decreased during the Holocene, contrary to the simulated warming results. The significant discrepancy between the reconstructed cooling and simulated warming reflect the "Holocene temperature conundrum" (Liu et al., 2014). Because the Tibetan Plateau is very sensitive to climate change, quantitative temperature records are likely to shed light on the "Holocene temperature conundrum" (Liu et al., 2014).

Over the past few decades, several biomarkers have been adopted to quantitatively reconstruct temperature variability in lacustrine sediments, such as the glycerol dialkyl glycerol tetraethers (GDGTs)–based proxies $TEX_{86}$ (the relative distribution of cyclopentane rings in isoprenoid GDGTs), MBT (the methylation of branched GDGTs [brGDGTs]), and CBT (the cyclization ratio of brGDGTs) and the alkenone proxies $U^{k}_{37}$, $U^{k'}_{37}$ and $U^{ks}_{37}$ (Günther et al., 2014; Wang et al., 2015; Hou et al., 2016). Although there is debate regarding the source of the brGDGTs (Blaga et al., 2010; Loomis et al., 2011), the brGDGT-based proxies MBT and CBT have been demonstrated to correlate with air temperature and soil pH, respectively (Weijers et al., 2007c; Zink et al., 2010; Pearson et al., 2011; Sun et al., 2011; Günther et al., 2014). Subsequently, the MBT index was simplified to MBT′ (Peterse et al., 2012). MBT/MBT′ and CBT have been adopted to reconstruct mean annual temperature variability as the soil bacteria that produce them are able to survive throughout the year (Weijers et al., 2006, 2007b, 2007c). Calibration between brGDGT indices and mean annual air temperature (MAAT) has been established by studying lake surface sediments on the Tibetan Plateau (Günther et al., 2014). In this study, we present records of temperature based on measurement of GDGTs and precipitation hydrogen isotopes based on sedimentary leaf waxes from the same Holocene sediment core from Aweng Co on the western side of the Tibetan Plateau. Combining temperature and precipitation isotope records from the same sediment core avoids problems caused by possible age offsets when synthesizing records obtained from different cores and sites. This article presents the first long, continuous, and quantitative temperature and precipitation isotope records from lake sediments on the WTP. The principal aims of the research are (1) to improve our understanding of the influence of the Indian summer monsoon and the midlatitude westerlies on the WTP during the Holocene; (2) to investigate the variation of mean annual temperature on the WTP, which currently is heavily biased toward winter temperature; and (3) to understand the nature of hydrologic changes on the WTP during the Holocene. The records of Aweng Co not only provide a picture of the hydrologic and thermal history of the WTP, but have also led to rethinking the impact of seasonality on proxy indicators. Furthermore, the quantitative temperature reconstruction can help to improve the accuracy of the climate models.

## MATERIALS AND METHODS

### Study site and sampling

Aweng Co (32°42′N–32°49′N, 81°38′E–81°48′E; 4427 m above sea level) is a closed carbonate-type saline lake located in Rutog County on the WTP. The lake has an area of 58.6 $km^2$, a maximum depth of 6 m, and a watershed area of 1750 $km^2$. The regional climate is classified as alpine subfrigid and is within the semiarid monsoon zone (Wang and Dou, 1998). A survey of the lake in 2012 indicated that the salinity of the surface lake water was 27.65 g/L, increasing to 28.16 g/L at the bottom. The pH of the lake water is 9.2. The lake is fed mainly by precipitation and by the Aweng Zangbo River, which originates from glacial meltwater. Records from a nearby meteorological station (Shiquanhe Town, data from 2011 to 2014) show that modern precipitation in the region is monsoonal, and that summer rainfall accounts for more than 80% of total annual precipitation. The only prior paleolimnological work at the site was a study of the vertical distribution of the bacterial community along a 20 cm gravity sediment core (Shi et al., 2014).

In 2011, a 567-cm-long sediment core, designated AWC2011-2, was retrieved using a UWITEC piston corer from a water depth of 4 m from the southeastern part of the lake (Fig. 1). The core was subsampled continuously at an interval of 1 cm, and all the samples were stored in a freezer prior to laboratory analysis.

### Chronology

Chronological control for core AWC2011-2 is based on $^{210}Pb$ and $^{137}Cs$ measurements of the uppermost 15 cm of the core, together with seven accelerator mass spectrometry (AMS) radiocarbon ages from the lower part of the core (Table 1). Because of the lack of terrestrial macrofossils, the AMS ages were obtained from bulk organic carbon. The depth of 9 cm was assigned an age of AD 1950 based on the $^{210}Pb$ data. The $^{14}C$ ages indicate that abrupt changes in the sedimentation rate occur at a depth of 309 cm. Changes in sedimentation rate may have an important impact on carbon reservoir ages (Zhou et al., 2014b), and therefore, the reservoir age may have changed at ~309 cm. Extrapolation of the uppermost three $^{14}C$ ages to the depth of 9 cm indicated a $^{14}C$ age of 4066 yr BP, which is regarded as the reservoir age for the sediment above 309 cm. Subsequently, we extrapolated the three $^{14}C$ ages down to the depth of 309 cm, which yielded a $^{14}C$ age of 2566 yr BP, while extrapolation of the lower four $^{14}C$ ages to 309 cm yielded an age of 5793 yr BP. Therefore, we took the difference (3227 yr) between the two ages as the reservoir age below 309 cm. This method of estimating the reservoir age below 309 cm follows the approach of Zhou et al. (2014b). Finally, the reservoir age–corrected $^{14}C$ data were calibrated to calendar ages, and we constructed an age model using the Bacon program (Fig. 2) (Blaauw and Christen, 2011). The reservoir ages may have changed significantly in the past (Hou et al., 2012), and therefore, the chronology for the core is tentative. Consequently, this article focuses on the long-term trends of temperature and precipitation isotope variation.

https://doi.org/10.1017/qua.2017.9 Published online by Cambridge University Press

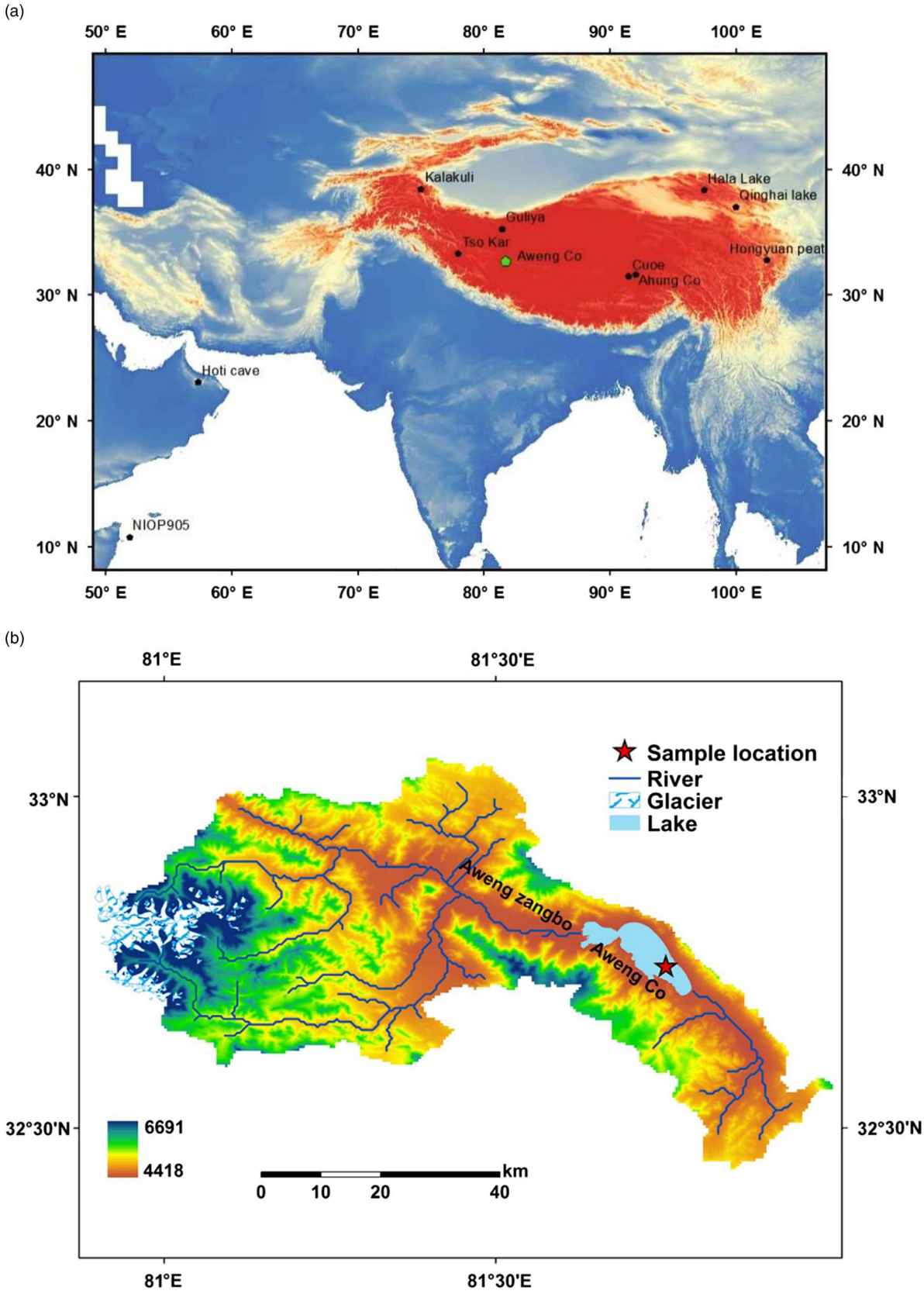


**Figure 1.** (color online) (a) Location of Aweng Co and other records mentioned in the text. (b) Catchment of Aweng Co.

https://doi.org/10.1017/qua.2017.9 Published online by Cambridge University Press

**Table 1**. Radiocarbon ages and reservoir age for core AWC2011-2.

| Lab ID | Depth (cm) | $^{14}$C age (yr BP) | Calibrated age (cal yr BP) | Reservoir age | Materials |
|---|---|---|---|---|---|
| BA130014 | 82.5 | 4635 ± 25 | 658–530 | 4066 | Bulk sediment |
| BA120318 | 130 | 5180 ± 20 | 1160–954 | 4066 | Bulk sediment |
| BA130016 | 280.5 | 6370 ± 25 | 2755–2314 | 4066 | Bulk sediment |
| BA120320 | 328 | 6430 ± 30 | 3657–3314 | 3227 | Bulk sediment |
| BA130017 | 380.5 | 7880 ± 35 | 5566–5046 | 3227 | Bulk sediment |
| BA120321 | 427 | 9710 ± 30 | 7498–7059 | 3227 | Bulk sediment |
| BA120322 | 566 | 13,895 ± 40 | 12763–10546 | 3227 | Bulk sediment |

## Analysis of deuterium-to-hydrogen ratios of sedimentary leaf waxes

Total lipids were extracted from freeze-dried lake sediments using ultrasonication and were further fractionated by flash column chromatography. Approximately 5 g of sediment samples was extracted with dichloromethane and methanol (volume ratio = 2:1) for three cycles of 15 min. Total lipid extracts were fractionated into neutral and acid fractions using liquid chromatography LC-$NH_2$ silica gel chromatography, eluted with dichloromethane:isopropanol (2:1 [v:v]) and ether: acetic acid (96:4 [v:v]), respectively. The acid fraction was methylated using anhydrous 2% HCl in methanol. Hydroxyl acids were removed using silica gel column chromatography (with dichloromethane as the solvent) to further purify the fatty acid methyl esters and avoid chromatographic coelution. Quantification and identification were carried out using gas chromatography and gas chromatography–mass spectrometry.

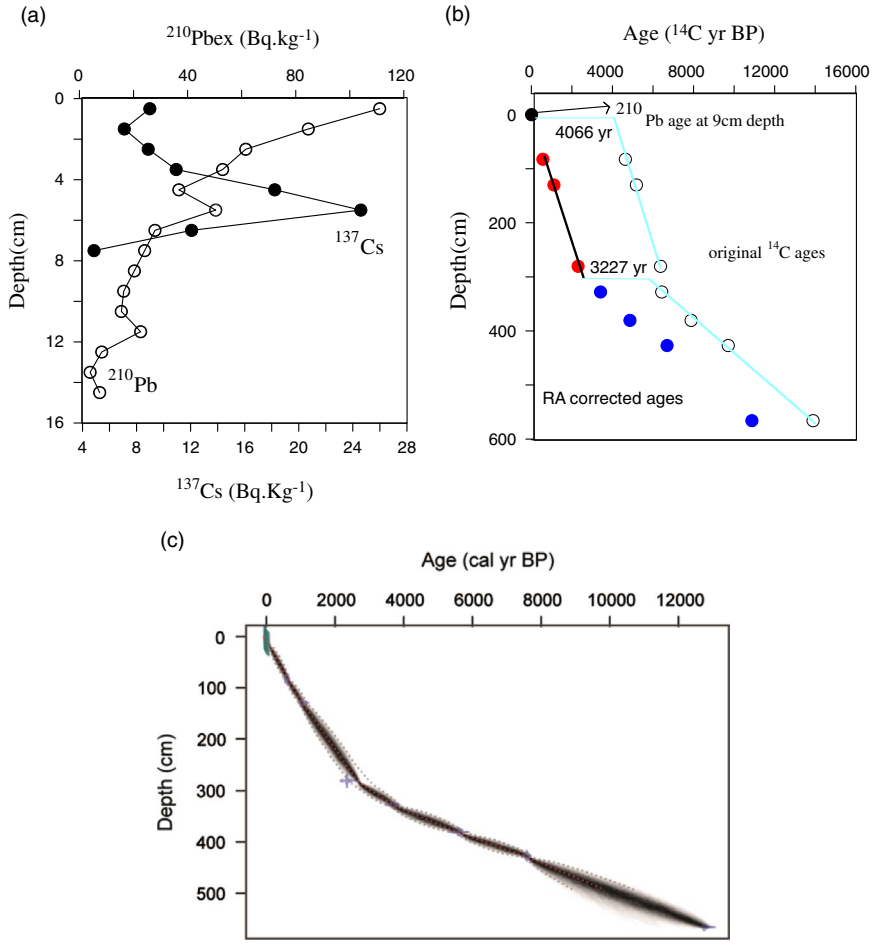


**Figure 2.** (color online) Age controls for Aweng Co sediment core AWC2011-2. (a) $^{210}$Pb-dating (open circles) and $^{137}$Cs-dating (solid circles) results. (b) Original $^{14}$C ages. The upper three $^{14}$C ages were corrected for an estimated reservoir age of 4066 yr, and the lower four $^{14}$C ages by an estimated reservoir age of 3227 yr. Open circles represent measured $^{14}$C ages, and solid circles represent $^{14}$C ages corrected for reservoir age. (c) Age-depth model for core AWC2012-2 using the "Bacon" program (Blaauw and Christen, 2011).

https://doi.org/10.1017/qua.2017.9 Published online by Cambridge University Press

An HP 6890 chromatograph interfaced to a Finnigan Delta+ XL stable isotope mass spectrometer through a high-temperature pyrolysis reactor was used for hydrogen isotopic analysis. The $H^{3+}$ factor was determined daily prior to sample analysis (average values of 2.0 during this study). The precision (1σ) of triplicate analyses was <2‰. The accuracy was routinely checked by injection of laboratory isotopic standards between every six measurements. The δD values obtained for individual acids (as methyl esters) were corrected by mathematically removing the isotopic contributions from the added group. The δD value of the added methyl group was determined by acidifying and then methylating (together with the samples) the disodium salt of succinic acid with a predetermined δD value (Huang et al., 2002).

## Analysis of GDGTs

Total lipids were extracted using ultrasonication and were further fractionated by flash column chromatography. Approximately 5 g of sediment samples was extracted with dichloromethane and methanol (volume ratio = 2:1) for three cycles of 15 min. Total lipid extracts were further chromatographed into several fractions. We used activated (for 2 h at 150°C) $Al_2O_3$ as the stationary phase and hexane:dichloromethane (9:1, 4 column volumes) to elute the nonpolar fraction and dichloromethane: methanol (1:1, 3 column volumes) to elute the polar fraction containing the GDGTs. After evaporation of the solvents, the polar fraction was redissolved in a high-performance liquid chromatography (HPLC)–grade mixture of hexane:isopropanol (99:1) at a concentration of 2 mg/mL. The dissolved polar fraction was finally filtered through a 0.4 μm Polytetrafluoroethylene (PTFE) filter attached to a 1 mL syringe.

GDGT analysis was performed using HPLC–atmospheric-pressure chemical ionization–mass spectrometry (APCI-MS) (Agilent 1260 HPLC, MS: 6100). Separation was done on a Grace Prevail Cyano (150 × 2.1 mm, 3 μm), maintained at 40°C. Sample injection volume was 20 μL. GDGTs were eluted with 90% A and 10% D for 5 min, followed by a linear gradient to 18% D in 45 min, where A is Hexane (Hex) and D is Hex: isopropanol (IPA) = 9:1. Detection was achieved using APCI-MS. Conditions were as follows: nebulizer pressure 60 psi, vaporizer temperature 400°C, flow rate of drying gas 6 L/min and temperature 200°C, capillary voltage 3600 V, and corona 5.5 μA. GDGTs were detected by selected ion monitoring. Quantification of GDGT compounds was achieved by integrating the areas of the $[M+H]^+$ peaks and comparing them with an external standard curve composed of known GDGTs.

# RESULTS

## Temperature variability during the past 12 ka

We used a recently developed calibration between MAAT and MBT′/CBT (Günther et al., 2014) to reconstruct the estimated MAAT variation at Aweng Co, as follows:

$$\mathrm{MAAT} = -3.84 + 9.84 * \mathrm{CBT} + 5.92 * \mathrm{MBT}'$$
$$\left(R^2 = 0.59, \mathrm{root-mean-square\ error} = 1.2^{\circ}\mathrm{C}\right), \quad \text{(Eq.1)}$$

where

$$MBT' = \frac{Ia + Ib + Ic}{Ia + Ib + Ic + IIa + IIb + IIc + IIIa} \quad \text{(Eq. 2)}$$

$$CBT = -\log\left(\frac{Ib + IIb}{Ia + IIa}\right) \quad \text{(Eq. 3)}$$

(Roman numerals in the equations after Peterse et al., 2012.)

Our reconstructed MAAT record at Aweng Co fluctuates between –5°C and 6.5°C, suggesting that temperature varied significantly during the Holocene on the WTP (Fig. 3). Note that the transfer function involves a temperature uncertainty

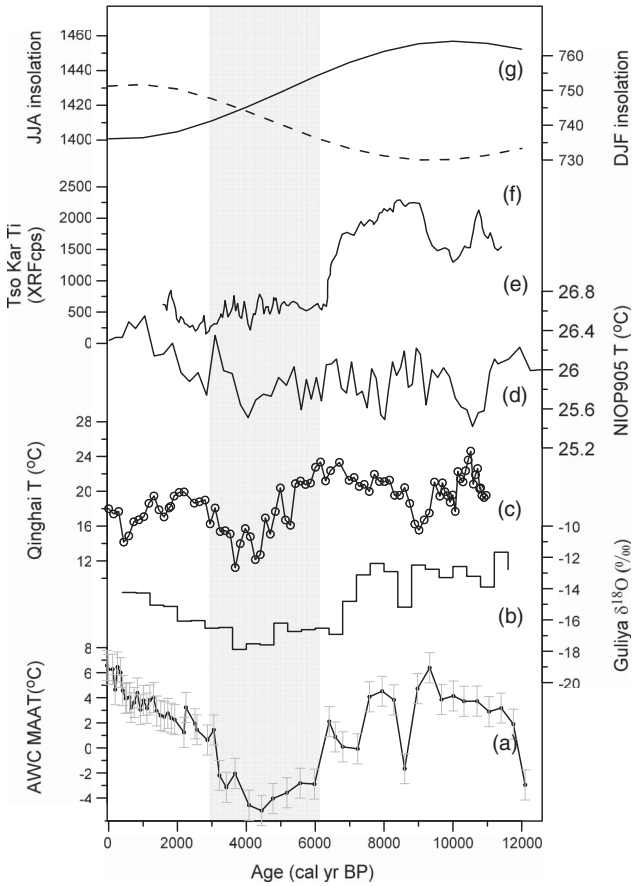


**Figure 3.** Holocene temperature records. (a) Glycerol dialkyl glycerol tetraether–inferred temperature record from Aweng Co (AWC). (b) $\delta^{18}O$ records from the Guliya ice core (Thompson et al., 1997). (c) Alkenone-based temperature record from Qinghai Lake (Hou et al., 2016). (d) Alkenone-based temperature record from core NIOP905 core from the western Arabian Sea (Huguet et al., 2006). (e) Ti concentration from Tso Kar (Wünnemann et al., 2010). (f) Mean winter (DJF) insolation at 30°N (Laskar et al., 2004). (g) Mean summer (JJA) insolation at 30°N (Laskar et al., 2004). MAAT, mean annual air temperature; XRF, X-ray fluorescence.

https://doi.org/10.1017/qua.2017.9 Published online by Cambridge University Press

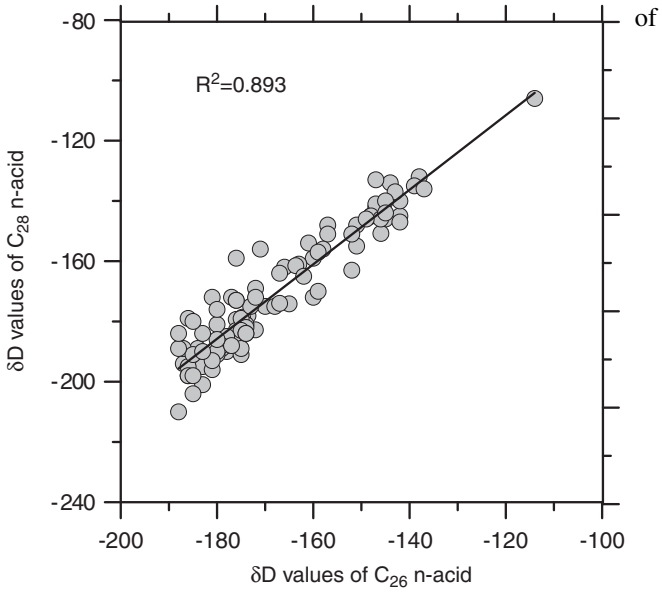


**Figure 4.** Relationship between the δD values of $C_{26}$ and $C_{28}$ *n*-alkanoic acids in the sediment core from Aweng Co.

1.2°C. From 12 to 9 ka, the MAAT increased gradually from −3°C to 6.4°C and then commenced a generally decreasing trend until 3 ka. After the cool interval between 6 and 3 ka, which is 3°C to ~4°C lower than during both the early and late Holocene, MAAT gradually increased to the current level (Fig. 3).

### Precipitation isotope variations over the past 9.8 ka

We measured deuterium-to-hydrogen (D/H) ratios for long-chain *n*-alkanoic acids at the sediment core AWC2011-2. Because the abundances of $C_{30}$ *n*-acids for most samples were very low, which may yield unrealistic D/H ratios, we present the D/H ratios of the $C_{26}$ and $C_{28}$ *n*-acids. The δD values of $C_{26}$ and $C_{28}$ *n*-acids are strongly correlated ($R^2 = 0.89$; Fig. 4), suggesting that both were produced by terrestrial plants. We calculated weighted average δD values of $C_{26}$ and $C_{28}$ *n*-acids ($\delta D_{wax}$) based on their abundance, in order to minimize the potential bias in isotope ratios between woody and herbaceous plants (Hou et al., 2007; Sachse et al., 2012; Li et al., 2015). The $\delta D_{wax}$ fluctuated significantly over the past 10 ka, ranging from −199‰ to −110‰ (Fig. 3). $\delta D_{wax}$ was relatively low between 6 and 9 ka and then maintained generally higher values between 2.5 and 6 ka. During the past 2.5 ka, the $\delta D_{wax}$ values were rather lower, averaging −182‰.

## DISCUSSION

### MBT′-CBT indices as a proxy for MAAT

GDGT-based proxies, such as $TEX_{86}$, MBT, and CBT indices, are increasingly used as proxies for paleotemperature reconstruction in marine and lake environments (Schouten et al., 2003; Powers et al., 2005; Blaga et al., 2009; Tierney and Russell, 2009; Loomis et al., 2011; Wang et al., 2012; Liu et al., 2013; Foster et al., 2016). $TEX_{86}$ likely works well in marine and very large lakes with high proportions of isoprenoid GDGTs. However, in medium and small lakes, the abundance of isoprenoid GDGTs is very low, and thus the use of $TEX_{86}$ is often not applicable (Blaga et al., 2010; Powers et al., 2010). However, brGDGTs are ubiquitous in lake sediments and have great potential as a continental paleothermometer (Blaga et al., 2009; Sinninghe Damsté et al., 2009; Tierney and Russell, 2009). brGDGTs were initially thought to be produced mainly by soil bacteria (Weijers et al., 2007c, 2009); however, further studies suggested in situ production of brGDGTs within lake systems (Sinninghe Damsté et al., 2009; Tierney and Russell, 2009; Blaga et al., 2010; Tierney et al., 2010; Loomis et al., 2011). Blaga et al. (2010) suggested that the mixed sources of the brGDGTs in lakes may influence the accuracy of MBT/CBT as proxies for temperature. However, despite their mixed sources, the distributions of brGDGTs has been demonstrated to be mainly influenced by temperature and pH (Zink et al., 2010; Pearson et al., 2011; Sun et al., 2011; Günther et al., 2014). Therefore, we adopted the MBT/CBT proxy as a quantitative proxy for past temperature changes. However, the temperature uncertainty is no less than 1.2°C because of the scatter inherited in the transfer function, error in measurements, and integration.

It has been demonstrated that the MBT-CBT indices are not biased to particular seasonal temperatures, and they likely reflect mean annual soil temperature (Weijers et al., 2007c, 2011), which has been used as a potential proxy for MAAT (Weijers et al., 2007a, 2007b; Schouten et al., 2008; Tierney and Russell, 2009; Pearson et al., 2011). An investigation into the turnover time of brGDGTs in soils showed that they have a turnover time of ~17 yr, implying that the brGDGT-based proxies should reflect long-term temperature variations (Weijers et al., 2010). Moreover, the transfer function for MBT′/CBT has been established via a comparison with MAAT (Günther et al., 2014). Therefore, we consider that our MBT′/CBT-based temperature at Aweng Co reflects changes in annual temperature on the WTP. It should be noted here that recently improved chromatography techniques enable us to separate the 5- and 6-methyl brGDGTs (De Jonge et al., 2014). The abundance of 6-methyl brGDGTs is well correlated with soil pH, and the exclusion of 6-methyl brGDGTs leads to a better correlation between MBT′ and MAAT (De Jonge et al., 2014; Yang et al., 2015). Although we did not discriminate 5- and 6-methyl brGDGTs in our measurements in 2014, we believe that our brGDGT-based temperature records should capture the long-term trend of temperature variation at Aweng Co.

### Variation of MAAT at Aweng Co during the past 12 ka

The MAAT at Aweng Co generally decreased from the early to middle Holocene, which is similar to most of

https://doi.org/10.1017/qua.2017.9 Published online by Cambridge University Press

the temperature records from the Tibetan Plateau and may be the result of the decreasing summer insolation (Fig. 3). The $\delta^{18}O$ record of the Guliya ice core is considered to reflect past temperature variations (Thompson et al., 1997). It indicates high temperatures during the early Holocene followed by a decrease to low temperatures during the middle Holocene. Overall, this pattern of Holocene temperature variation is very similar to the Aweng Co MAAT record. The titanium concentration record at Tso Kar, which reflects changing detrital fluxes from the catchment into the lake, is strongly linked to glacier melting (Wünnemann et al., 2010). The record indicates a high lake level during the early Holocene as a result of enhanced glacier melting because of high temperatures, and a lower lake level during the middle Holocene and hence less glacier melting because of low temperatures. Two recent alkenone-based temperature records from Lake Qinghai also suggest a cooling trend from the early to the middle Holocene (Wang et al., 2015; Hou et al., 2016). The similarity of these records suggests that they reflect the same climatic forcing—that is, decreasing summer insolation in the Northern Hemisphere during the early to middle Holocene (Fig. 3).

However, the late Holocene part of the MAAT record from Aweng Co differs from the records from monsoonal regions (Fig. 3) in that it increases gradually to the present. This pattern resembles the alkenone-based temperature record in sediment core NIOP905 from the Somalia Basin in the western Arabian Sea (Huguet et al., 2006). Aweng Co and the Somalia Basin belong to the same climate system (Chen, D., personal communication, 2016). Temperature proxies could potentially be biased because of different growing seasons of the biomarker source organisms (Huguet et al., 2006). Seasonal variations in phytoplankton production are less pronounced in tropical low latitudes, and a data–model comparison study suggests that the Holocene warming in the tropics was attributable to the increasing boreal winter insolation (Lorenz et al., 2006). Thus, the alkenone-based late Holocene temperature increase in core NIOP905 was attributed to the orbitally driven insolation increase during the boreal winter. Note the nearby meteorological station (Shiquanhe, data from 2011 to 2014) indicates that monthly average temperatures at or below 0°C in this region last for 7 months. Therefore, the MAAT record from Aweng Co was largely modulated by winter temperature. We consider that the late Holocene warming at Aweng Co may be attributed to increasing winter temperature in response to increasing winter insolation. Changes in the seasonality between summer and winter insolation, caused by the changing Earth orbital parameters, is one of the most important forcing mechanisms of Holocene climate change (Lorenz et al., 2006). During the early Holocene (12–6 ka) when summer insolation in the Northern Hemisphere was relatively high, the MAAT record at Aweng Co would likely be biased by summer insolation. During the middle Holocene (6–3 ka), when summer insolation decreased and winter insolation gradually increased, the MAAT record decreased significantly, suggesting that the MAAT was less biased toward summer insolation. The middle Holocene cooling on the WTP is confirmed by the Paleoclimate Modelling Intercomparison Project Phase II models, which generated much colder than modern winter temperatures and relatively lower mean annual temperatures over the WTP because of seasonal changes in insolation in the Northern Hemisphere (Jiang et al., 2012). As the insolation seasonality decreased during the late Holocene, MAAT in the Aweng Co gradually increased (Fig. 3).

## Hydrologic changes at Aweng Co during the Holocene

Terrestrial higher plants are the dominant source of long-chain *n*-alkanoic acids ($C_{26}$, $C_{28}$, and $C_{30}$) in lake sediments, and their δD values reflect changes in the δD of continental precipitation ($\delta D_p$) (Huang et al., 2004; Sachse et al., 2006; Hou et al., 2008; Tierney et al., 2008; Garcin et al., 2012; Guenther et al., 2013). Investigations of modern precipitation isotopes suggest that in the south and eastern Tibetan Plateau, which is mainly influenced by the monsoon, the $\delta D_p$ variation reflects changes in precipitation amount. In contrast, in the north and western Tibetan Plateau, which is influenced by the midlatitude westerlies, the $\delta D_p$ variation is mainly affected by temperature (Tian et al., 2007; Gao et al., 2011; Yao et al., 2013). Data from a nearby meteorological station (Shiquanhe, from 2011 to 2014) show that modern precipitation in the study region is monsoonal, with summer rainfall accounting for more than 80% of the annual total precipitation. A study by Tian et al. (2007) indicates that the northern limit of the summer monsoon is located to the north of the Yalong Zangbo River, in the middle of the Tibetan Plateau, at around 34°N to ~35°N. Based on the study results, we consider that Aweng Co is influenced by the Indian summer monsoon and that the $\delta D_p$ variations at the site mainly reflect changes in precipitation amount.

Millennial-scale variations in $\delta D_{wax}$ at Aweng Co during the early to middle Holocene exhibit features similar to the $\delta^{18}O$ record of speleothems from Dongge Cave and Qunf Cave, suggesting a monsoonal influence during the study interval period (Fig. 5) (Dykoski et al., 2005; Fleitmann et al., 2007). The strong Indian monsoon during the early Holocene from about 9–6 ka brought heavy precipitation to Aweng Co, and the $\delta D_{wax}$ values were lower. Subsequently, the monsoon weakened at around 6 cal ka BP, and this conclusion is supported by the record of sedimentary total organic carbon content at Cuoe Lake and by the carbonate content of Ahung Co (Morrill et al., 2006; Wu et al., 2006). The humification index record from the Hongyuan peatland, reflecting the degree of peat decomposition, is strongly influenced by local conditions of wetness and temperature and is commonly used as a proxy for the intensity of the Indian summer monsoon (Wang et al., 2004; Yu et al., 2006). During the early to middle Holocene, a decrease in the degree of humification of the Hongyuan peatland suggests a weakening of the Indian summer monsoon, which is similar to the Aweng Co $\delta D_{wax}$ record. In addition, the $\delta D_{wax}$ record from Lake

https://doi.org/10.1017/qua.2017.9 Published online by Cambridge University Press

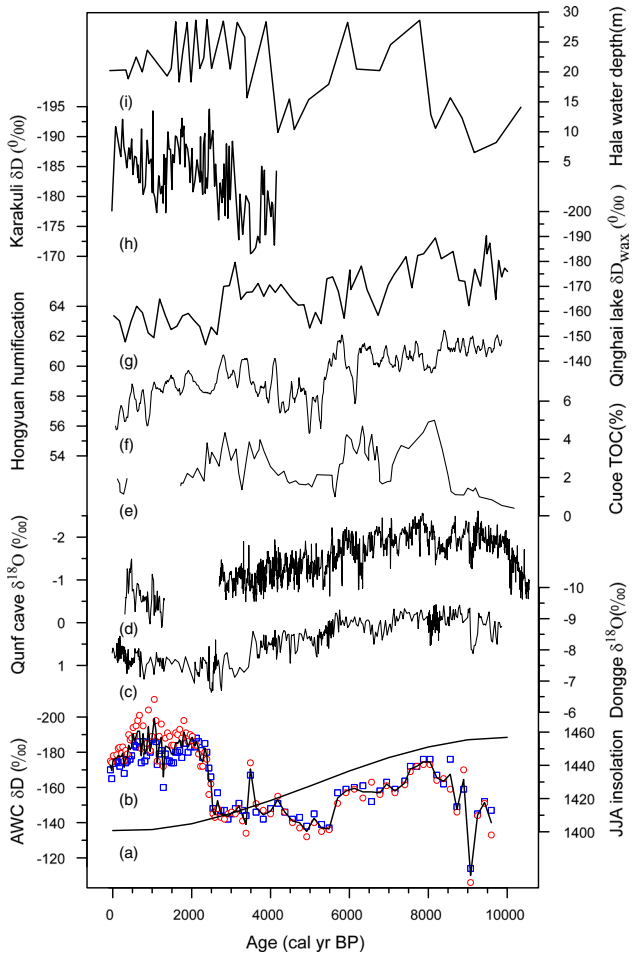


**Figure 5.** Comparison of the precipitation isotope records from Aweng Co (AWC) with records of monsoonal variation since 10 ka. (a) Summer insolation (JJA) at 30°N (Laskar et al., 2004). (b) Hydrogen isotope record of *n*-alkanoic acids at Aweng Co (red open circles represent $C_{28}$ *n*-alkanoic acids, blue diamonds represent $C_{26}$ *n*-alkanoic acids, and the solid line is the weighted average). (c) $\delta^{18}O$ record from Dongge Cave (Dykoski et al., 2005). (d) $\delta^{18}O$ record from Qunf Cave (Fleitmann et al., 2007). (e) Total organic carbon (TOC) content at Cuoe Lake (Wu et al., 2006). (f) Humification index at Hongyuan peatland (Yu et al., 2006). (g) Hydrogen isotope record of *n*-alkanoic acids from Lake Qinghai (Thomas et al., 2016). (h) Hydrogen isotope record of *n*-alkanoic acids from Lake Karakuli (Aichner et al., 2015). (i) Estimated water depth changes in Hala Lake (Yan and Wünnemann, 2014). (For interpretation of the references to color in this figure legend, the reader is referred to the web version of this article.)

Qinghai, which reflects changes in growing season moisture source, also indicates a reduction in summer monsoon precipitation during the Holocene (Thomas et al., 2016).

In addition to changes in summer monsoon intensity, the meridional displacement of the seasonal cycle of the midlatitude westerlies relative to the present day may also influence precipitation δD (Nagashima et al., 2011; Kana et al., 2013; Chiang et al., 2015). During the early Holocene when the summer insolation was high, the midlatitude westerly jet shifted northward onto the Tibetan Plateau earlier in the summer, suggesting an earlier northward transition of the summer monsoon and a longer summer monsoon season (Chiang et al., 2015). The longer summer monsoon season probably brought more precipitation to Aweng Co. Later, during the middle Holocene when summer insolation weakened, the summer season was relatively short and the monsoon influence was probably weak on the Tibetan Plateau, thereby bringing less precipitation to Aweng Co.

Most of the records indicate that the summer monsoon further weakened during the late Holocene. For example, a phase of drying after 3 ka at Cuoe Lake indicates that the influence of the Indian monsoon diminished in that region during the late Holocene (Wu et al., 2006). Sedimentological and $\delta D_{wax}$ data from Paru Co (southeastern Tibetan Plateau) provide a Holocene perspective of Indian summer monsoon, and the results indicate that the summer monsoon trended toward drier conditions to the present since 5.2 ka (Bird et al., 2014). Besides, the $\delta^{18}O$ record of speleothems from Dongge Cave and Qunf Cave, the carbonate content of Ahung Co, the humification index record from the Hongyuan peatland, and the $\delta D_{wax}$ record from Lake Qinghai all suggest a long-term trend of decreased monsoon intensity during the Holocene (Fleitmann et al., 2003, 2007; Wang et al., 2004; Dykoski et al., 2005; Morrill et al., 2006; Thomas et al., 2016). However, the δD values at Aweng Co exhibit an abrupt decrease at ~3 ka. Clearly, this does not reflect the direct influence of summer monsoon rainfall given the scale of the decreased monsoonal influence at that time. In addition, variations in temperature cannot fully explain the observed very large isotopic variability (up to 56‰) in such a short period. Rather, changes in the moisture source probably contributed to the observed hydrogen isotope variations at Aweng Co. During the late Holocene when the monsoon weakened, the midlatitude westerlies would have been able to penetrate into the region (An et al., 2012), supplying precipitation with relatively depleted hydrogen isotope ratios (Yao et al., 2013). This is supported by the δD record of a sediment core from Lake Kalakuli, the values of which were relatively low during the late Holocene suggesting the influence of the midlatitude westerlies (Aichner et al., 2015). In addition, records of changing water depth at Hala Lake (in the western Qilian Mountains, Qinghai Province), based on ostracod assemblages, stable isotopes, and sediment geochemical properties from four sediment cores from different water depths, suggest that the late Holocene was characterized by extremely unstable hydrologic conditions and by rapid fluctuations in lake water depth at the site, which were mainly controlled by changes in westerly driven effective moisture (Yan and Wünnemann, 2014) (Fig. 5). Despite the influence of the midlatitude westerlies on Lake Kalakuli and Hala Lake, it is difficult to attribute the lower $\delta D_{wax}$ values to the westerly precipitation during the late Holocene as temperature increased at the same time. The imprint of the midlatitude westerlies in the Aweng Co precipitation isotope record is unclear based on our current data.

https://doi.org/10.1017/qua.2017.9 Published online by Cambridge University Press

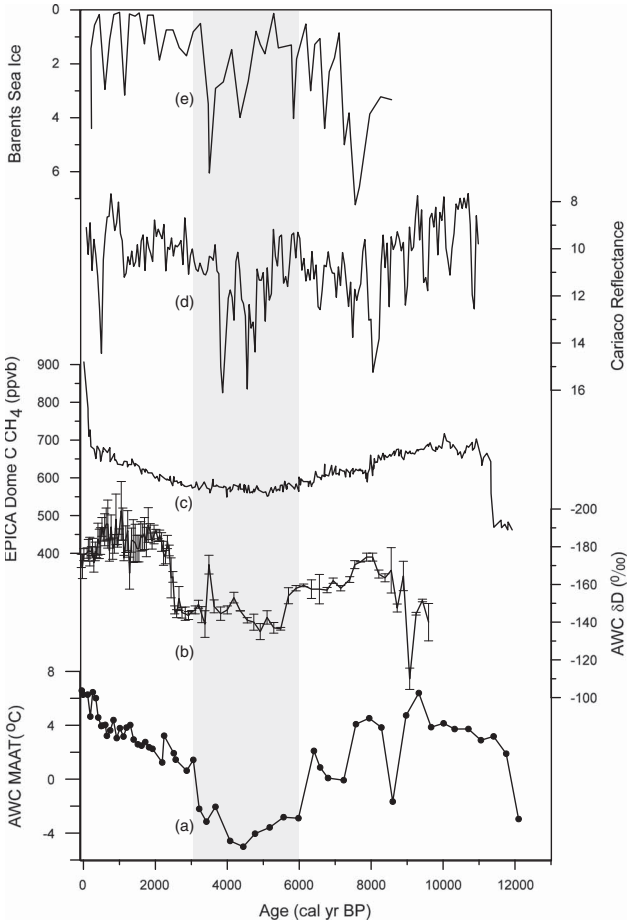


**Figure 6.** Temperature and hydrologic records from Aweng Co (AWC) compared with records of atmospheric $CH_4$, sediment reflectance from the Cariaco Basin, and sea ice in the Barents Sea. (a) Glycerol dialkyl glycerol tetraether–inferred mean annual air temperature (MAAT) record from Aweng Co. (b) Leaf wax hydrogen isotope record from Aweng Co. (c) Atmospheric methane record from the EPICA Dome C ice core (Loulergue et al., 2008). (d) Sea ice concentration in the Barents Sea (de Vernal et al., 2013). (e) Sediment reflectance in the Cariaco Basin (Peterson et al., 2000).

A comparison with the temperature record from Aweng Co indicates that increased temperature, as well as the related glacier melting, may also have contributed to the abrupt decrease of precipitation isotopes at Aweng Co. Elevated temperatures during the late Holocene would have accelerated melting of the local glacier, thus resulting in the increased influx of meltwater to Aweng Co via the Aweng Zangbo River. Previous results have demonstrated isotopic fractionation effects associated with processes of glacier melting (Zhou et al., 2014a). The stable isotope ratios of glacier ice are usually lower than that of the rainfall because of the low temperature of the precipitation that would result in significant isotopic fractionation. For example, $\delta^{18}O$ and $\delta D$ of precipitation in Nyalam are clearly more enriched than that of the nearby Dasuopu glacier, Xixiabangma (Tian et al., 2005). In addition, the higher atmospheric $CH_4$ concentration during the late Holocene supports the glacier melting hypothesis (Fig. 6). Thus, the observed decreased precipitation isotopes during the late Holocene may be attributed to the accelerated glacier melting because of the elevated MAAT.

The MAAT variability at Aweng Co resembles the record of $CH_4$ concentration in the European Project for Ice Coring in Antarctica (EPICA) ice cores (Loulergue et al., 2008), implying that the MAAT variability on the WTP was linked to variations in the concentration of atmospheric $CH_4$. Changes in temperature and in water table variations are the main controls on $CH_4$ emissions (Walter and Heimann, 2000). Consequently, it has been suggested that high-resolution methane records can be used as a proxy of Northern Hemisphere temperature fluctuations on a millennial scale (Delmotte et al., 2004; Loulergue et al., 2008). Changes in temperature resulting in thawing and refreezing of the soil active layer, as well as changes in the extent of seasonal snow cover, all influence $CH_4$ emissions. Variations in rainfall caused by changes in the strength of the monsoon can also lead to variations in atmospheric methane concentration (Ruddiman, 2000). A strong monsoon results in heavy rainfall within the region of influence, causing saturation of the ground and increases in the amount of standing water in bogs and creating an environment suitable for generating methane. During the early Holocene, the strong monsoon and the high temperature in the WTP would have contributed to the $CH_4$ emissions as a result of an increase in the areas of standing water and the thawing of frozen soil. During the colder interval of the middle Holocene, large amounts of methane were stored in the frozen ground. The weakened monsoon brought little rainfall to the region, and the dry environment would have reduced the release of $CH_4$ to the atmosphere. The high temperatures and resulting generation of large amounts of meltwater would have thawed the soil resulting in the emission of a large amount of methane to the atmosphere during the late Holocene.

The sediment reflectance record from of the Cariaco Basin, reflecting shifts in the Intertropical Convergence Zone (ITCZ) (Fig. 6) (Peterson et al., 2000), indicates that the ITCZ moved southward and that the Indian summer monsoon weakened continuously from 6 to 3 ka. In addition, an abrupt positive shift in the $\delta^{18}O$ values of stalagmites at Hoti Cave (northern Oman) at ~6 ka reflects an abrupt southward movement of the ITCZ and a decrease in the dynamics of Indian summer monsoon precipitation (Fleitmann et al., 2007), which is further supported by a depositional hiatus from 5.2 to 2.5 ka (Fleitmann et al., 2007). During the middle to late Holocene, the ITCZ migrated southward and monsoonal precipitation gradually decreased.

A coupling of atmospheric and oceanic heat fluxes from the North Atlantic would have affected the extent of sea ice in the Barents Sea (Voronina et al., 2001; de Vernal et al., 2013). The observed southward extension of sea ice in the Barents Sea at 3.5 and 4.3 ka (de Vernal et al., 2013) indicating an overall decrease in Atlantic water inputs to the Arctic Ocean, which is responsible for climatic amplification in the Northern Hemisphere via the sea ice albedo feedback, had a worldwide climatic effect (Voronina et al., 2001; Renssen et al., 2005, 2006; de Vernal et al., 2013). The extension of the sea ice possibly indicates cooling in the moisture

https://doi.org/10.1017/qua.2017.9 Published online by Cambridge University Press

source region for the midlatitude westerlies that would have potentially reached Aweng Co during the middle Holocene.

## CONCLUSIONS

A quantitative temperature record and a precipitation isotope record for the Holocene have been constructed from analysis of MBT′, CBT, and sedimentary leaf waxes at Aweng Co, a small saline lake located on the WTP. The changes in the seasonality of insolation and fluctuations of the Indian monsoon were the major forcing mechanisms of climate change at Aweng Co during the Holocene. Aweng Co experienced a relatively warm and wet early Holocene (10 to ~6 ka), a cool and dry middle Holocene (6 to ~3 ka), and a relatively warm and wet late Holocene. Decreasing summer insolation and a weakened Indian monsoon contributed to the cool and dry middle Holocene. This cool and dry interval reflects a teleconnection with cold events in the North Atlantic Ocean and a southward shift of the ITCZ, as well as a decreased atmospheric methane concentration. During the early and middle Holocene, precipitation at Aweng Co was mainly influenced by fluctuations in the intensity and seasonal movement of the summer monsoon on the Tibetan Plateau. However, during the late Holocene when the Indian monsoon weakened, the precipitation isotope record at Aweng Co may have been influenced by glacier melting as a result of increased temperatures during the late Holocene.

## ACKNOWLEDGMENTS

This work was supported by the "Strategic Priority Research Program (B) (Grant No. XDB01020300)" of the Chinese Academy of Sciences and by the Natural Science Foundation of China (Grant Nos. 41072120, 41321061).

## REFERENCES

Aichner, B., Feakins, S.J., Lee, J.E., Herzschuh, U., Liu, X., 2015. High-resolution leaf wax carbon and hydrogen isotopic record of the late Holocene paleoclimate in arid Central Asia. *Climate of the Past* 11, 619–633.

An, Z., Colman, S.M., Zhou, W., Li, X., Brown, E.T., Jull, A.J., Cai, Y., *et al*., 2012. Interplay between the Westerlies and Asian monsoon recorded in Lake Qinghai sediments since 32 ka. *Scientific Reports* 2, 619.

Bird, B.W., Polisar, P.J., Lei, Y., Thompson, L.G., Yao, T., Finney, B.P., Bain, D.J., Pompeani, D.P., Steinman, B.A., 2014. A Tibetan lake sediment record of Holocene Indian summer monsoon variability. *Earth and Planetary Science Letters* 399, 92–102.

Blaauw, M., Christen, J.A., 2011. Flexible paleoclimate age-depth models using an autoregressive gamma process. *Bayesian Analysis* 6, 457–474.

Blaga, C.I., Reichart, G.-J., Heiri, O., Sinninghe Damsté, J.S., 2009. Tetraether membrane lipid distributions in water-column particulate matter and sediments: a study of 47 European lakes along a north–south transect. *Journal of Paleolimnology* 41, 523–540.

Blaga, C.I., Reichart, G.-J., Schouten, S., Lotter, A.F., Werne, J.P., Kosten, S., Mazzeo, N., Lacerot, G., Sinninghe Damsté, J.S., 2010. Branched glycerol dialkyl glycerol tetraethers in lake sediments: can they be used as temperature and pH proxies? *Organic Geochemistry* 41, 1225–1234.

Bradley, R.S., Keimig, F.T., Diaz, H.F., 2004. Projected temperature changes along the American cordillera and the planned GCOS network. *Geophysical Research Letters* 31, L16210.

Bradley, R.S., Vuille, M., Diaz, H.F., Vergara, W., 2006. Threats to water supplies in the tropical Andes. *Science* 312, 1755–1756.

Chiang, J.C.H., Fung, I.Y., Wu, C.H., Cai, Y., Edman, J.P., Liu, Y., Day, J.A., Bhattacharya, T., Mondal, Y., Labrousse, C.A., 2015. Role of seasonal transitions and westerly jets in East Asian paleoclimate. *Quaternary Science Reviews* 108, 111–129.

De Jonge, C., Hopmans, E.C., Zell, C.I., Kim, J.-H., Schouten, S., Sinninghe Damsté, J.S., 2014. Occurrence and abundance of 6-methyl branched glycerol dialkyl glycerol tetraethers in soils: implications for palaeoclimate reconstruction. *Geochimica et Cosmochimica Acta* 141, 97–112.

Delmotte, M., Chappellaz, J., Brook, E., Yiou, P., Barnola, J.M., Goujon, C., Raynaud, D., Lipenkov, V.I., 2004. Atmospheric methane during the last four glacial-interglacial cycles: rapid changes and their link with Antarctic temperature. *Journal of Geophysical Research: Atmospheres* 109, D12104.

de Vernal, A., Hillaire-Marcel, C., Rochon, A., Fréchette, B., Henry, M., Solignac, S., Bonnet, S., 2013. Dinocyst-based reconstructions of sea ice cover concentration during the Holocene in the Arctic Ocean, the northern North Atlantic Ocean and its adjacent seas. *Quaternary Science Reviews* 79, 111–121.

Dykoski, C., Edwards, R., Cheng, H., Yuan, D., Cai, Y., Zhang, M., Lin, Y., Qing, J., An, Z., Revenaugh, J., 2005. A high-resolution, absolute-dated Holocene and deglacial Asian monsoon record from Dongge Cave, China. *Earth and Planetary Science Letters* 233, 71–86.

Fleitmann, D., Burns, S.J., Mangini, A., Mudelsee, M., Kramers, J., Villa, I., Neff, U., *et al*., 2007. Holocene ITCZ and Indian monsoon dynamics recorded in stalagmites from Oman and Yemen (Socotra). *Quaternary Science Reviews* 26, 170–188.

Fleitmann, D., Burns, S.J., Mudelsee, M., Neff, U., Kramers, J., Mangini, A., Matter, A., 2003. Holocene forcing of the Indian monsoon recorded in a stalagmite from southern Oman. *Science* 300, 1737–1739.

Foster, L.C., Pearson, E.J., Juggins, S., Hodgson, D.A., Saunders, K.M., Verleyen, E., Roberts, S.J., 2016. Development of a regional glycerol dialkyl glycerol tetraether (GDGT)–temperature calibration for Antarctic and sub-Antarctic lakes. *Earth and Planetary Science Letters* 433, 370–379.

Gao, J., Masson-Delmotte, V., Yao, T., Tian, L., Risi, C., Hoffmann, G., 2011. Precipitation water stable isotopes in the south Tibetan Plateau: observations and modeling. *Journal of Climate* 24, 3161–3178.

Garcin, Y., Schwab, V.F., Gleixner, G., Kahmen, A., Todou, G., Séné, O., Onana, J.-M., Achoundong, G., Sachse, D., 2012. Hydrogen isotope ratios of lacustrine sedimentary n-alkanes as proxies of tropical African hydrology: insights from a calibration transect across Cameroon. *Geochimica et Cosmochimica Acta* 79, 106–126.

Guenther, F., Aichner, B., Siegwolf, R., Xu, B., Yao, T., Gleixner, G., 2013. A synthesis of hydrogen isotope variability and its hydrological significance at the Qinghai–Tibetan Plateau. *Quaternary International* 313–314, 3–16.

Günther, F., Thiele, A., Gleixner, G., Xu, B., Yao, T., Schouten, S., 2014. Distribution of bacterial and archaeal ether lipids in soils and surface sediments of Tibetan lakes: implications for GDGT-based proxies in saline high mountain lakes. *Organic Geochemistry* 67, 19–30.

Hou, J., D'Andrea, W.J., Huang, Y., 2008. Can sedimentary leaf waxes record D/H ratios of continental precipitation? Field, model, and experimental assessments. *Geochimica et Cosmochimica Acta* 72, 3503–3517.

Hou, J., D'Andrea, W.J., Liu, Z., 2012. The influence of $^{14}C$ reservoir age on interpretation of paleolimnological records from the Tibetan Plateau. *Quaternary Science Reviews* 48, 67–79.

Hou, J., D'Andrea, W.J., MacDonald, D., Huang, Y., 2007. Hydrogen isotopic variability in leaf waxes among terrestrial and aquatic plants around Blood Pond, Massachusetts (USA). *Organic Geochemistry* 38, 977–984.

Hou, J., Huang, Y., Zhao, J., Liu, Z., Colman, S., An, Z., 2016. Large Holocene summer temperature oscillations and impact on the peopling of the northeastern Tibetan Plateau. *Geophysical Research Letters* 43, 1323–1330.

Huang, Y., Shuman, B., Wang, Y., Webb, T., 2002. Hydrogen isotope ratios of palmitic acid in lacustrine sediments record late Quaternary climate variations. *Geology* 30, 1103–1106.

Huang, Y., Shuman, B., Wang, Y., Webb, T., 2004. Hydrogen isotope ratios of individual lipids in lake sediments as novel tracers of climatic and environmental change: a surface sediment test. *Journal of Paleolimnology* 31, 363–375.

Huguet, C., Kim, J.H., Sinninghe Damsté, J.S., Schouten, S., 2006. Reconstruction of sea surface temperature variations in the Arabian Sea over the last 23 kyr using organic proxies ($TEX_{86}$ and $U^{K7}_{37}$). *Paleoceanography* 21, PA3003.

Immerzeel, W., 2008. Historical trends and future predictions of climate variability in the Brahmaputra basin. *International Journal of Climatology* 28, 243–254.

Immerzeel, W.W., Beek, L.P.H., Van , Bierkens, M.F.P., 2010. Climate change will affect the Asian water towers. *Science* 328, 1382–1385.

Jiang, D., Lang, X., Tian, Z., Wang, T., 2012. Considerable model–data mismatch in temperature over China during the mid-Holocene: results of PMIP simulations. *Journal of Climate* 25, 4135–4153.

Kana, N., Ryuji, T., Shin, T., 2013. Westerly jet-East Asian summer monsoon connection during the Holocene. *Geochemistry, Geophysics, Geosystems* 14, 5041–5053.

Laskar, J., Robutel, P., Joutel, F., Gastineau, M., Correia, A., Levrard, B., 2004. A long-term numerical solution for the insolation quantities of the Earth. *Astronomy & Astrophysics* 428, 261–285.

Li, X., Liang, J., Hou, J., Zhang, W., 2015. Centennial-scale climate variability during the past 2000 years on the central Tibetan Plateau. *Holocene* 25, 892–899.

Liu, W., Wang, H., Zhang, C.L., Liu, Z., He, Y., 2013. Distribution of glycerol dialkyl glycerol tetraether lipids along an altitudinal transect on Mt. Xiangpi, NE Qinghai-Tibetan Plateau, China. *Organic Geochemistry* 57, 76–83.

Liu, X., Cheng, Z., Yan, L., Yin, Z.Y., 2009. Elevation dependency of recent and future minimum surface air temperature trends in the Tibetan Plateau and its surroundings. *Global & Planetary Change* 68, 164–174.

Liu, Z., Zhu, J., Rosenthal, Y., Zhang, X., Otto-Bliesner, B.L., Timmermann, A., Smith, R.S., Lohmann, G., Zheng, W., Timm, O.E., 2014. The Holocene temperature conundrum. *Proceedings of the National Academy of Sciences of the United States of America* 111, E3501–E3505.

Loomis, S.E., Russell, J.M., Sinninghe Damsté, J.S., 2011. Distributions of branched GDGTs in soils and lake sediments from western Uganda: implications for a lacustrine paleothermometer. *Organic Geochemistry* 42, 739–751.

Lorenz, S.J., Kim, J.H., Rimbu, N., Schneider, R.R., Lohmann, G., 2006. Orbitally driven insolation forcing on Holocene climate trends. *Paleoceanography* 21, PA1002.

Loulergue, L., Schilt, A., Spahni, R., Masson-Delmotte, V., Blunier, T., Lemieux, B., Barnola, J.M., Raynaud, D., Stocker, T.F., Chappellaz, J., 2008. Orbital and millennial-scale features of atmospheric CH4 over the past 800,000 years. *Nature* 453, 383–386.

Morrill, C., Overpeck, J.T., Cole, J.E., Liu, K.-b., Shen, C., Tang, L., 2006. Holocene variations in the Asian monsoon inferred from the geochemistry of lake sediments in central Tibet. *Quaternary Research* 65, 232–243.

Nagashima, K., Tada, R., Tani, A., Sun, Y., Isozaki, Y., Toyoda, S., Hasegawa, H., 2011. Millennial-scale oscillations of the westerly jet path during the last glacial period. *Journal of Asian Earth Sciences* 40, 1214–1220.

Pearson, E.J., Juggins, S., Talbot, H.M., Weckström, J., Rosén, P., Ryves, D.B., Roberts, S.J., Schmidt, R., 2011. A lacustrine GDGT-temperature calibration from the Scandinavian Arctic to Antarctic: renewed potential for the application of GDGT-paleothermometry in lakes. *Geochimica et Cosmochimica Acta* 75, 6225–6238.

Peterse, F., van der Meer, J., Schouten, S., Weijers, J.W., Fierer, N., Jackson, R.B., Kim, J.-H., Sinninghe Damsté, J.S., 2012. Revised calibration of the MBT–CBT paleotemperature proxy based on branched tetraether membrane lipids in surface soils. *Geochimica et Cosmochimica Acta* 96, 215–229.

Peterson, L.C., Haug, G.H., Hughen, K.A., Röhl, U., 2000. Rapid changes in the hydrologic cycle of the tropical Atlantic during the last glacial. *Science* 290, 1947–1951.

Powers, L., Werne, J.P., Vanderwoude, A.J., Sinninghe Damsté, J.S., Hopmans, E.C., Schouten, S., 2010. Applicability and calibration of the $TEX_{86}$ paleothermometer in lakes. *Organic Geochemistry* 41, 404–413.

Powers, L.A., Johnson, T.C., Werne, J.P., Castañeda, I.S., Hopmans, E.C., Sinninghe Damsté, J.S., Schouten, S., 2005. Large temperature variability in the southern African tropics since the Last Glacial Maximum. *Geophysical Research Letters* 32, L08706.

Renssen, H., Goosse, H., Fifchefet, T., 2005. Contrasting trends in North Atlantic deep-water formation in the Labrador Sea and Nordic Seas during the Holocene. *Geophysical Research Letters* 32, L08711.

Renssen, H., Goosse, H., Muscheler, R., 2006. Coupled climate model simulation of Holocene cooling events: oceanic feedback amplifies solar forcing. *Climate of the Past* 2, 79–90.

Ruddiman, W.F., 2000. *Earth's Climate: Past and Future*. W.H. Freeman, New York.

Sachse, D., Billault, I., Bowen, G.J., Chikaraishi, Y., Dawson, T.E., Feakins, S.J., Freeman, K.H., *et al*., 2012. Molecular paleohydrology: interpreting the hydrogen-isotopic composition of lipid biomarkers from photosynthesizing organisms. *Annual Review of Earth and Planetary Sciences* 40, 221–249.

Sachse, D., Radke, J., Gleixner, G., 2006. δD values of individual *n*-alkanes from terrestrial plants along a climatic gradient – implications for the sedimentary biomarker record. *Organic Geochemistry* 37, 469–483.

Schiemann, R., Lüthi, D., Schär, C., 2009. Seasonality and interannual variability of the westerly jet in the Tibetan Plateau region. *Journal of Climate* 22, 2940–2957.

https://doi.org/10.1017/qua.2017.9 Published online by Cambridge University Press

Schouten, S., Baas, M., Hopmans, E.C., Sinninghe Damsté, J.S., 2008. An unusual isoprenoid tetraether lipid in marine and lacustrine sediments. *Organic Geochemistry* 39, 1033–1038.

Schouten, S., Hopmans, E.C., Forster, A., van Breugel, Y., Kuypers, M.M., Sinninghe Damsté, J.S., 2003. Extremely high sea-surface temperatures at low latitudes during the middle Cretaceous as revealed by archaeal membrane lipids. *Geology* 31, 1069–1072.

Shi, Y., Sun, H., Liu, Y., Hou, J., Zhu, L., Chu, H., 2014. Vertical distribution of bacterial community in sediments of freshwater lake Puma Yumco and saline lake AWongco on the Tibetan Plateau. *Microbiology China* 41, 2379–2387.

Sinninghe Damsté, J.S., Ossebaar, J., Abbas, B., Schouten, S., Verschuren, D., 2009. Fluxes and distribution of tetraether lipids in an equatorial African lake: constraints on the application of the $TEX_{86}$ palaeothermometer and BIT index in lacustrine settings. *Geochimica et Cosmochimica Acta* 73, 4232–4249.

Sun, Q., Chu, G., Liu, M., Xie, M., Li, S., Ling, Y., Wang, X., Shi, L., Jia, G., Lü, H., 2011. Distributions and temperature dependence of branched glycerol dialkyl glycerol tetraethers in recent lacustrine sediments from China and Nepal. *Journal of Geophysical Research: Biogeosciences* 116, G01008.

Thomas, E.K., Huang, Y., Clemens, S.C., Colman, S.M., Morrill, C., Wegener, P., Zhao, J., 2016. Changes in dominant moisture sources and the consequences for hydroclimate on the northeastern Tibetan Plateau during the past 32 kyr. *Quaternary Science Reviews* 131, 157–167.

Thompson, L.G., Yao, T., Davis, M., Henderson, K., Mosley-Thompson, E., Lin, P.-N., Beer, J., Synal, H.-A., Cole-Dai, J., Bolzan, J., 1997. Tropical climate instability: the last glacial cycle from a Qinghai-Tibetan ice core. *Science* 276, 1821–1825.

Tian, L., Yao, T., MacClune, K., White, J.W.C., Schilla, A., Vaughn, B., Vachon, R., Ichiyanagi, K., 2007. Stable isotopic variations in west China: a consideration of moisture sources. *Journal of Geophysical Research: Atmospheres* 112, D10112.

Tian, L., Yao, T., White, J.W.C., Yu, W., Wang, N., 2005. Westerly moisture transport to the middle of Himalayas revealed from the high deuterium excess. *Chinese Science Bulletin* 50, 1026–1030.

Tierney, J.E., Russell, J.M., 2009. Distributions of branched GDGTs in a tropical lake system: implications for lacustrine application of the MBT/CBT paleoproxy. *Organic Geochemistry* 40, 1032–1036.

Tierney, J.E., Russell, J.M., Eggermont, H., Hopmans, E., Verschuren, D., Damsté, J.S., 2010. Environmental controls on branched tetraether lipid distributions in tropical East African lake sediments. *Geochimica et Cosmochimica Acta* 74, 4902–4918.

Tierney, J.E., Russell, J.M., Huang, Y., Damste, J.S., Hopmans, E.C., Cohen, A.S., 2008. Northern Hemisphere controls on tropical southeast African climate during the past 60,000 years. *Science* 322, 252–255.

Voronina, E., Polyak, L., Vernal, A.D., Peyron, O., 2001. Holocene variations of sea-surface conditions in the southeastern Barents Sea, reconstructed from dinoflagellate cyst assemblages. *Journal of Quaternary Science* 16, 717–726.

Walter, B.P., Heimann, M., 2000. A process-based, climate-sensitive model to derive methane emissions from natural wetlands: application to five wetland sites, sensitivity to model parameters, and climate. *Global Biogeochemical Cycles* 14, 745–765.

Wang, H., Hong, Y., Zhu, Y., Hong, B., Lin, Q., Xu, H., Leng, X., Mao, X., 2004. Humification degrees of peat in Qinghai-Xizang Plateau and palaeoclimate change. *Chinese Science Bulletin* 49, 514–519.

Wang, H., Liu, W., Zhang, C.L., Wang, Z., Wang, J., Liu, Z., Dong, H., 2012. Distribution of glycerol dialkyl glycerol tetraethers in surface sediments of Lake Qinghai and surrounding soil. *Organic Geochemistry* 47, 78–87.

Wang, S., Dou, H., 1998. *China Lake Records*. Science Press, Beijing.

Wang, Z., Liu, Z., Zhang, F., Fu, M., An, Z., 2015. A new approach for reconstructing Holocene temperatures from a multi-species long chain alkenone record from Lake Qinghai on the north-eastern Tibetan Plateau. *Organic Geochemistry* 88, 50–58.

Weijers, J.W.H., Bernhardt, B., Peterse, F., Werne, J.P., Dungait, J.A.J., Schouten, S., Sinninghe Damsté, J.S., 2011. Absence of seasonal patterns in MBT–CBT indices in mid-latitude soils. *Geochimica et Cosmochimica Acta* 75, 3179–3190.

Weijers, J.W.H., Blaga, C.I., Werne, J.P., Sinninghe Damsté, J.S., 2009. Microbial membrane lipids in lake sediments as a paleothermometer. *PAGES news* 17, 102–104.

Weijers, J.W.H., Schefuß, E., Schouten, S., Sinninghe Damsté, J.S., 2007a. Coupled thermal and hydrological evolution of tropical Africa over the last deglaciation. *Science* 315, 1701–1704.

Weijers, J.W.H, Schouten, S., Hopmans, E.C., Geenevasen, J.A., David, O.R., Coleman, J.M., Pancost, R.D., Sinninghe Damsté, J.S., 2006. Membrane lipids of mesophilic anaerobic bacteria thriving in peats have typical archaeal traits. *Environmental Microbiology* 8, 648–657.

Weijers, J.W.H., Schouten, S., Sluijs, A., Brinkhuis, H., Sinninghe Damsté, J.S., 2007b. Warm arctic continents during the Palaeocene–Eocene thermal maximum. *Earth and Planetary Science Letters* 261, 230–238.

Weijers, J.W.H., Schouten, S., van den Donker, J.C., Hopmans, E.C., Sinninghe Damsté, J.S., 2007c. Environmental controls on bacterial tetraether membrane lipid distribution in soils. *Geochimica et Cosmochimica Acta* 71, 703–713.

Weijers, J.W.H., Wiesenberg, G.L.B., Bol, R., Hopmans, E.C., Pancost, R.D., 2010. Carbon isotopic composition of branched tetraether membrane lipids in soils suggest a rapid turnover and a heterotrophic life style of their source organism(s). *Biogeosciences* 7, 2959–2973.

Wu, Y., Lücke, A., Jin, Z., Wang, S., Schleser, G.H., Battarbee, R.W., Xia, W., 2006. Holocene climate development on the central Tibetan Plateau: a sedimentary record from Cuoe Lake. *Palaeogeography, Palaeoclimatology, Palaeoecology* 234, 328–340.

Wünnemann, B., Demske, D., Tarasov, P., Kotlia, B.S., Reinhardt, C., Bloemendal, J., Diekmann, B., Hartmann, K., Krois, J., Riedel, F., 2010. Hydrological evolution during the last 15kyr in the Tso Kar lake basin (Ladakh, India), derived from geomorphological, sedimentological and palynological records. *Quaternary Science Reviews* 29, 1138–1155.

Yan, D., Wünnemann, B., 2014. Late Quaternary water depth changes in Hala Lake, northeastern Tibetan Plateau, derived from ostracod assemblages and sediment properties in multiple sediment records. *Quaternary Science Reviews* 95, 95–114.

Yang, H., Lu, X., Ding, W., Lei, Y., Dang, X., Xie, S., 2015. The 6-methyl branched tetraethers significantly affect the performance of the methylation index (MBT′), in soils from an altitudinal transect at Mount Shennongjia. *Organic Geochemistry* 82, 42–53.

Yao, T., Masson-Delmotte, V., Gao, J., Yu, W., Yang, X., Risi, C., Sturm, C., *et al.*, 2013. A review of climatic controls on $\delta^{18}O$ in precipitation over the Tibetan Plateau: observations and simulations. *Reviews of Geophysics* 51, 525–548.

Yao, T., Thompson, L., Yang, W., Yu, W., Gao, Y., Guo, X., Yang, X., Duan, K., Zhao, H., Xu, B., 2012. Different glacier status with atmospheric circulations in Tibetan Plateau and surroundings. *Nature Climate Change* 2, 663–667.

Yu, X., Zhou, W., Franzen, L.G., Xian, F., Cheng, P., Jull, A.T., 2006. High-resolution peat records for Holocene monsoon history in the eastern Tibetan Plateau. *Science in China Series D* 49, 615–621.

Zhou, S., Wang, Z., Joswiak, D.R., 2014a. From precipitation to runoff: stable isotopic fractionation effect of glacier melting on a catchment scale. *Hydrological Processes* 28, 3341–3349.

Zhou, W., Cheng, P., Jull, A.J.T., Lu, X., An, Z., Wang, H., Zhu, Y., Wu, Z., 2014b. $^{14}C$ chronostratigraphy for Qinghai Lake in China. *Radiocarbon* 56, 143–155.

Zink, K.-G., Vandergoes, M.J., Mangelsdorf, K., Dieffenbacher-Krall, A.C., Schwark, L., 2010. Application of bacterial glycerol dialkyl glycerol tetraethers (GDGTs) to develop modern and past temperature estimates from New Zealand lakes. *Organic Geochemistry* 41, 1060–1066.

https://doi.org/10.1017/qua.2017.9 Published online by Cambridge University Press